Cancer Chemother Pharmacol (1999) 43: 213–220

ORIGINAL ARTICLE

Alastair H. Kyle · Andrew I. Minchinton

Measurement of delivery and metabolism of tirapazamine to tumour tissue using the multilayered cell culture model

Received: 6 February 1998 / Accepted: 29 June 1998

Abstract *Purpose:* Efficient extravascular penetration is essential for the optimal activity of most anticancer drugs and is particularly relevant to bioreductive cytotoxins which target hypoxic cells that can be located distal to functional blood vessels within tumours. Tirapazamine (3-amino-1,2,4-benzotriazine-1,4-di-N-oxide; Triazone; SR 259075; formerly SR 4233) is a lead bioreductive cytotoxin currently undergoing clinical evaluation. It exhibits preferential cytotoxicity towards cells at reduced oxygen tension, and could complement existing anticancer therapies where hypoxic cells are believed to constitute a refractory population. We assessed the ability of tirapazamine to penetrate tumour tissue using an in vitro multilayered cell culture (MCC) model. *Methods:* Diffusion of tirapazamine through oxic and hypoxic multilayered cell cultures composed of SiHa, human cervical carcinoma cells, was measured using a dual reservoir diffusion apparatus from which samples were quantified via HPLC. Drug concentration kinetics from both reservoirs were analysed using a mathematical model for diffusion and metabolism within the MCC. Results were then applied to a second mathematical model which described extravascular drug penetration within a tumour cord, the sheath of cells surrounding a blood vessel. *Results:* The diffusion coefficient of tirapazamine within SiHa MCCs was determined as $7.0 \pm 0.5 \times 10^{-7}$ cm^2/s and the maximal metabolic rate for hypoxic MCCs, V_{max}, as 1.5 ± 0.4 μM/s. The thickness of individual tissue cultures was determined by diffusion of tritiated water (HTO). A linear relationship was shown to exist between tissue thickness and the inverse of permeability to HTO. Experimental results were used to simulate drug distribution within a tumour cord. These simulations indicate that, when tirapazamine is administered via intravenous infusion, a stable tirapazamine distribution throughout the cord occurs within 15 min with cells most peripheral to the blood vessel exposed to only 10% of the blood drug concentration. Under these conditions, the simulations predict cell kill to be limited to the first 75 μm of tissue surrounding a blood vessel. *Conclusions:* This study indicates that extravascular penetration of tirapazamine to peripheral cells existing at low oxygen tension may be limited by the metabolism of tirapazamine by more proximal cells existing at moderate oxygen tension. Simulations found that tirapazamine reached only 10% of the blood concentration at cells most peripheral to blood vessels. These results indicate that tirapazamine would be significantly cytotoxic only to cells located within ~75 μm of blood vessels. Further MCC-based modelling of extravascular drug penetration would serve as a means of identifying new antitumour agents with location-specific activity.

Key words Tirapazamine · Multilayered cell culture · Drug diffusion/penetration · Drug delivery · Tumour modelling

This research was supported by grants from the National Cancer Institute of Canada with funds from the Canadian Cancer Society and the BC Health Research Foundation

A.H. Kyle · A.I. Minchinton (✉)
Department of Medical Biophysics, B.C. Cancer Research Centre, 601 West 10th Avenue, Vancouver, B.C. V5Z 1L3, Canada
Tel.: +1-604-877-6182; Fax: +1-604-877-6002;
E-mail: minc@unixg.ubc.ca

Introduction

The molecular characteristics of new and existing pharmaceuticals determine not only their potency to interact with specific macromolecules (e.g. receptors, enzymes, DNA) but also their delivery to target cells. For most anticancer drugs to be optimally effective towards solid tumours they need to reach as many tumour cells as possible at therapeutic concentrations. Passage of a drug through tumour tissue is determined by its physicochemical characteristics (size, partition coefficient, pK, etc.) as well as its stability, binding affinity to macromolecules and rate of metabolism as it traverses the cellular and paracellular spaces. The capacity of drugs to

penetrate the perivascular compartment of tumours has received little attention because of the lack of relevant quantitative models. In this study we examined the ability of a new bioreductive cytotoxin, tirapazamine, to penetrate tumour tissue using a novel in vitro model.

Tirapazamine (3-amino-1,2,4-benzotriazine-1,4-di-N-oxide; Triazone; SR 259075; formerly SR 4233) is a bioreductive cytotoxin exhibiting preferential toxicity to cells at reduced oxygen tension. It is believed that under hypoxic conditions tirapazamine is reductively metabolized to a cytotoxic free radical intermediate which causes DNA strand breaks and cell death [14]. Hypoxic cells in suspension culture are ~40 times more sensitive to tirapazamine than corresponding well-oxygenated cells [23], though a much smaller differential in sensitivity has been observed in multicellular spheroids and tumours [8–10]. Tirapazamine enhances radiation- and chemotherapy-based antitumour activity in experimental animals [3, 7, 24], and is the lead compound in this new class of anticancer agents. It is presently undergoing clinical evaluation [2, 4, 11, 18]. Tirapazamine could complement clinical radiotherapy and chemotherapy by sterilizing cells at reduced oxygen tension which can be located distal to functional tumour blood vessels. Radiation- and chemotherapy-based treatments are more effective at killing cells proximal to tumour blood vessels. In the case of radiation therapy this is because oxygen tension determines radiation sensitivity and cells distal to blood vessels can be hypoxic and therefore resistant to radiation-induced cytotoxicity. Chemotherapy agents are geometrically diluted as they diffuse radially away from blood vessels reducing their effectiveness, and many chemotherapy agents are selectively active against cycling cells, and tumour cells existing distant from blood vessels at low oxygen tension are likely to be quiescent. The effective passage of tirapazamine from the blood, through the blood vessel and to all the cells comprising the tumour, is an absolute prerequisite for its optimal effectiveness.

Multilayered cell culture (MCC) has been recently developed to provide a quantitative way of assessing drug distribution profiles within tumour tissue. The MCC model comprises a disc of cells grown on a permeable membrane; its culture and characteristics have been described elsewhere [5, 15]. MCCs are complementary to other multicellular culture systems such as spheroids in that they share many features with tumour tissue growing in vivo [8–10, 16, 20]. To grow MCCs, a monolayer of cells is seeded onto a permeable membrane, submerged in stirred medium and cultured to the desired thickness. Unlike spheroids, MCCs can be oriented to separate two reservoirs, thereby allowing the quantification of drug passage from one reservoir to the other. In addition to determining a drug's diffusion coefficient in the tissue, experiments can also determine the rate of drug consumption by the culture. This ability to simultaneously measure drug flux and metabolism in a 'tissue-like' environment permits a comprehensive assessment of drug penetration to be made.

We measured the rate of diffusion and metabolism of tirapazamine within MCCs and have applied the results to simulate tirapazamine distribution within solid tumours assuming a corded architecture [21]. Data from drug flux experiments were analysed using a mathematical model based on Fickean diffusion and Michaelis-Menten enzyme kinetics. Experimental estimates for the rate of diffusion and metabolism within MCCs were then applied to a second mathematical model describing a corded tumour architecture. Using this model, simulations were carried out to examine the extent of drug penetration within solid tumour tissue.

Materials and methods

Chemicals and materials

Tirapazamine was obtained from Sterling Winthrop (Collegeville, Pa.). Tritiated water (HTO) was purchased from Amersham Life Science (Oakville, ON, Canada). Collagen rat tail type I and trypsin/EDTA were purchased from Sigma (Oakville, ON, Canada). Minimum essential medium (MEM) with Earle's salts and fetal bovine serum (FBS) were purchased from GIBCO/BRL (Burlington, ON, Canada). Millicell CM 0.4-μm 12-mm tissue culture inserts were purchased from Millipore (Nepean, ON, Canada).

Cells

SiHa (human cervix squamous cell carcinoma) cells were purchased from American Type Culture Collection. Monolayer cells were grown in MEM with 10% FBS in tissue culture plates (Falcon 3003, Franklin Lakes, NJ, USA.) and passaged every 4 to 5 days by trypsinization upon reaching confluence.

MCCs

The surface of the tissue culture insert membrane was coated with 100 μl 0.75 mg/ml collagen solution made up by dissolving 25 mg collagen in 50 μl 1 *M* HCl and then diluting with 33.3 ml 60% ethanol. The membranes were allowed to dry overnight and approximately 2×10^5 cells in MEM containing 10% FBS were then inoculated onto the coated surface of the membrane in a volume of 400 μl and incubated for 2–4 h to allow the cells to attach. Silicone O-rings placed around the inserts were used to support them in a frame with slots for six inserts [15]. The frame was then completely immersed in 120 ml stirred medium. Cultures were incubated for up to 8 days with continual gassing (5% O_2, 5% CO_2 and 90% N_2) at 37.5 °C. The medium was changed daily after the first 3 days. After diffusion experiments, MCCs were sandwiched between 1-mm layers of Tissue-Tek OCT embedding medium (Miles, Ind.) and frozen. A portion of each MCC was then cut out using a 7-mm diameter cork borer, and 10-μm cryostat sections were made from the portions. Thickness was measured microscopically using a calibrated ocular reticle.

Diffusion

Experiments were performed using a dual reservoir diffusion apparatus (Fig. 1). Prior to the experiment, MCCs were selected and visually assessed for uniformity. The cultures were then placed in the diffusion apparatus with 6–10 ml medium per reservoir. For oxic experiments the cultures were equilibrated for 1 h (with gassing at 5 ml/min with 5% O_2, 5% CO_2, 90% N_2 at 37.5 °C.

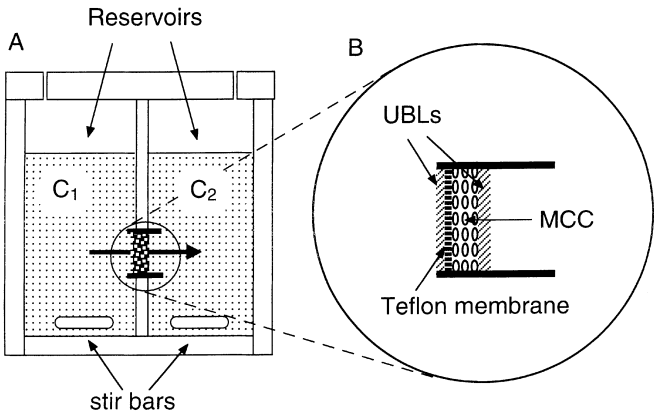

Fig. 1A,B Diffusion apparatus schematic. **A** Two reservoirs are connected by the tissue culture. The temperature, gassing and stirring of each chamber is controlled throughout the experiments. The medium can be sampled via access ports from the top to determine drug concentrations C_1 and C_2. The *arrow* indicates drug flux when $C_1 > C_2$. **B** Configuration of cell insert within the apparatus. The impediments to diffusion are two unstirred boundary layers (UBLs), the Teflon support membrane and the multilayered culture

Hypoxic experiments were left to equilibrate for 2.5 h with gassing at 10 ml/min with 5% CO_2, 95% N_2 at 37.5 °C. Using an Eppendorf oxygen sensor (Eppendorf pO_2 Histograph, Hamburg, Germany), oxygen levels in the medium measured less than 0.5% after 2.5 h of gassing. Experiments were then carried out over 6–10 h using a starting concentration of 100 μ*M* tirapazamine and 0.5 μCi/ml HTO. Samples of 50 μl were taken (Hamilton, Reno, Nev.) over increasing time intervals. HPLC and scintillation counting were carried out immediately after each sampling. Following the experiments, 10-μm cryostat sections were made to confirm MCC thickness.

HPLC

Chromatographic analysis was carried out with Waters equipment (Mississauga, ON, Canada), including a model 510 pump, model 712 WISP injector and model 996 photodiode array detector. A Symmetry C18 column (3.9 × 150 mm) was used for sample separation. Sample preparation was carried out by adding 5 μl of a 40% aqueous solution of $ZnSO_4$ to each 50-μl medium sample which was then mixed with 100 μl methanol. After shaking, the precipitate was pelleted by centrifugation at 2.5×10^3 *g* for 10 min and 140 μl of the supernatant was removed and placed in glass HPLC vials. Samples of 40 μl were injected using a mobile phase of an acetonitrile/H_2O mixture (0.13:0.87) flowing at 1.5 ml/min whereby tirapazamine eluted after 1.8 min. Absorbance detection was carried out at 460 nm. The metabolites SR 4330 and SR 4317 were separated from the tirapazamine peak with retention times of 5.3 and 6.2 min, respectively.

Scintillation counting

Scintillation counting of samples of each reservoir were carried out using a LKB/Wallac 1214 Rackbeta liquid scintillation counter. Samples were prepared by adding 50 μl samples to 1 ml of 30% Scintisafe™ purchased from Fisher Scientific; Nepean, Ont., Canada. Vials were shaken vigorously and then left for 2 h before performing scintillation counting over a 5-min time interval. Counting efficiencies were about 40%.

Tissue modelling

Drug flux through the tissue was quantified using a modified version of a diffusion-reaction model previously used for MCCs [12]. In brief, the MCC is modelled as a homogeneous disc of thickness λ and area A, which is divided into a number of layers. Fick's second law of diffusion then relates drug flux to concentration gradients across each layer. When experiments were carried out under hypoxic conditions, drug metabolism in each layer within the MCC was modelled using the Michaelis-Menten equation for an enzymatically reduced substrate. The equation for the complete diffusion-reaction model is written as:

$$\frac{\partial C}{\partial t} = D\frac{\partial^2 C}{\partial x^2} - \frac{V_{max} C}{K_m + C} \quad (1)$$

where D (cm^2/s) is the effective diffusion coefficient, V_{max} (μ*M*/s) is the maximum rate of enzymatic drug metabolism, K_m (μ*M*) is the concentration of tirapazamine at which drug metabolism is half maximal and C is the drug concentration within the culture which is a function of both position x, and time, t.

The boundary condition relating flux into and out of the disc to concentration changes in each reservoir is written as:

$$\frac{dC_{1,2}}{dt} = \left(\frac{DA}{V}\right)\left.\frac{\partial C}{\partial x}\right|_{x=0,\lambda} \quad (2)$$

where A is the surface area of the culture, V is the reservoir volume, and $C_1(x = 0)$ and $C_2(x = \lambda)$ are the drug concentrations in the two reservoirs.

A complete description of drug flux must also account for the effects of the Teflon support membrane of the tissue culture insert and unstirred boundary layers (UBLs) on drug fluxes. Mathematically, these effects are accounted for by adding layers to the tissue model in which the drug's diffusion coefficient is modified.

Equations 1 and 2 were solved numerically using a modified Crank-Nicolson implicit integration scheme [6]. This facilitated the removal of experimental artifacts such as the additional diffusive layers and the effect of sampling on reservoir volumes. Computations were carried out on a Power Macintosh using the C programming language.

Data analysis

Estimates of the model parameters D and V_{max} were obtained using standard nonlinear chi-square minimization fitting techniques [17]. Data from both reservoirs were fitted simultaneously in order to ensure a mass balance in terms of flux into and out of the tissue and drug lost through metabolism. The parameter K_m was set to a value of 75 μ*M* as previously reported [22].

Results

Diffusion through the Teflon membrane of the tissue culture insert

Initial experiments were carried out to determine the permeability of the Teflon tissue culture inserts to HTO and tirapazamine. For HTO this yielded $D = 9.6 \pm 0.3 \times 10^{-6}$ cm^2/s and for tirapazamine $4.2 \pm 0.3 \times 10^{-6}$ cm^2/s (insert thickness, 30 μm). These results were used in all subsequent data analysis to correct for the effect of the tissue culture inserts and UBLs. Typically they adjusted measured permeabilities by less than 10% for HTO and by 2–5% for tirapazamine.

Mathematically, the effect of the tissue culture insert and UBLs is described as a single layer to the side of the MCC where the Teflon membrane is located. From the geometry of the culture inserts (Fig. 1), we expect that most of the contribution from the UBLs is located on the side of the tissue culture opposite the Teflon membrane. For tirapazamine, which is subject to cell metabolism under hypoxic conditions, grouping both UBLs to one side will skew the results. However, the effect of the UBLs contributes only fractionally to the total 2–5% correction of the effect of the plastic membrane and UBLs when grouped together. Hence, any error introduced by this correcting procedure is limited to a fraction of this value. For HTO, grouping the UBLs to one side of the culture is not a problem since the order of the diffusion layers is not important when there is no metabolism.

Assessment of MCC thickness

Figure 2 shows data from a typical experiment where HTO diffuses through an MCC, the results of which were used to determine the tissue culture thickness. Both curves were fitted simultaneously to the mathematical diffusion model to obtain the permeability of the MCC to HTO. Knowing the diffusion coefficient of HTO in the MCCs, allowed the MCC thickness to be determined from measurement of permeability (described below). Fitting both data sets simultaneously allowed Co, the initial concentration, to be made a parameter of the fit.

Figure 3 shows a plot of culture thickness versus the inverse of permeability to HTO. Permeability was determined using diffusion experiments such as those shown in Fig. 2, and thickness was determined through cryostat sectioning. The data indicate a linear relationship over the range 70–300 μm which confirms that the diffusion coefficient for HTO is effectively constant over this range. Care was taken to avoid using cultures whose thickness fell above this range as they generally exhibited a necrotic central region. The data were fitted to a line with the *y*-intercept forced through zero. Results yielded $D_{HTO} = \text{slope} = 3.45 \pm 0.1 \times 10^{-6}$ cm^2/s with $r = 0.95$. If the data were not linear over the region it would indicate the diffusion coefficient varied with changes in the tissue environment due to increased thickness or age; this was not observed. In further experiments, the result for D_{HTO} was used to determine culture thickness using $\lambda = D_{HTO}/P_{HTO}$ where P_{HTO} was measured for each culture. This yielded an accurate measure of the effective thickness of each culture reflecting an averaged value over the entire MCC. Generally, cryostat sectioning gave uncertainties of 10–20% while the uncertainty in determining P_{HTO} was less than 5%.

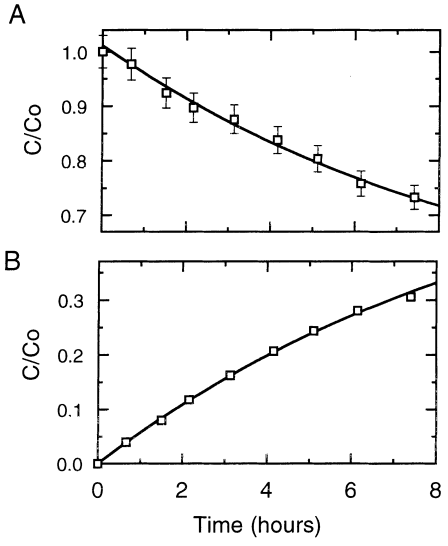

Fig. 2A,B Typical data for diffusion of tritiated water (HTO); **A** concentration in the donating reservoir, **B** concentration in the receiving reservoir. Both data sets were fitted simultaneously to the diffusion model, $P = 1.7 \times 10^{-4}$ cm/s; thickness was determined to be ~200 μm. *Error bars* indicate the estimated 3% measurement error and a 0.003 constant error; for **B** *error bars* are smaller than the data points

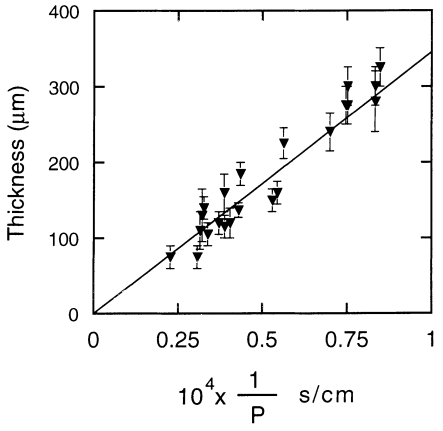

Fig. 3 Plot of MCC thickness versus the inverse of permeability to HTO. Each point is from a separate experiment where MCC permeability was determined followed by measurement of thickness via cryostat sectioning. *Error bars* indicate the estimated variation in MCC thickness using four to six sections. The data show a linear relationship which indicates that the diffusion coefficient remained constant over the range of thicknesses. The data are fitted with a straight line forced through zero

Diffusion of tirapazamine

Figure 4 shows typical experimental results where tirapazamine diffuses through a 85-μm thick MCC under oxic conditions. Fitting results from a series of such experiments, with cultures ranging in thickness from 80 to 110 μm, yielded a value for $D_{Tira} = 6.7 \times 10^{-7}$ cm^2/s with a standard deviation of 0.4×10^{-7} cm^2/s ($n = 4$). For these experiment, using thin, well-oxygenated cultures, the metabolic rate parameter, V_{max}, was set to zero and the results of the fit indicated no detectable loss of tirapazamine to metabolism. A substantial level of drug metabolism would have skewed the fit, and it

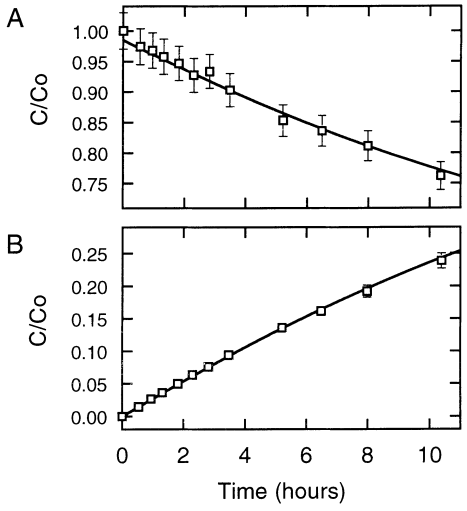

Fig. 4A,B Diffusion of tirapazamine under oxic conditions ($pO_2 = 40$ mmHg). Drug concentrations in donating (**A**) and receiving (**B**) reservoirs from one experiment are shown. Both data sets were fitted simultaneously, with V_{max} set to zero. *Error bars* indicate the estimated 3% measurement error plus 0.003 constant error

would not have been possible to satisfy both data sets simultaneously. In addition, neither of the two major tirapazamine metabolites, SR 4330 and SR 4317, were detected during HPLC measurement of tirapazamine levels.

The diffusion of tirapazamine through a fully hypoxic, 140-μm MCC is shown in Fig. 5. Results from several experiments, with cultures ranging in thickness from 80 to 180 μm gave values for $D_{Tira} = 7.3 \times 10^{-7}$ cm^2/s with a standard deviation of 0.5×10^{-7} cm^2/s ($n = 7$), and $V_{max} = 1.5$ μM/s with a

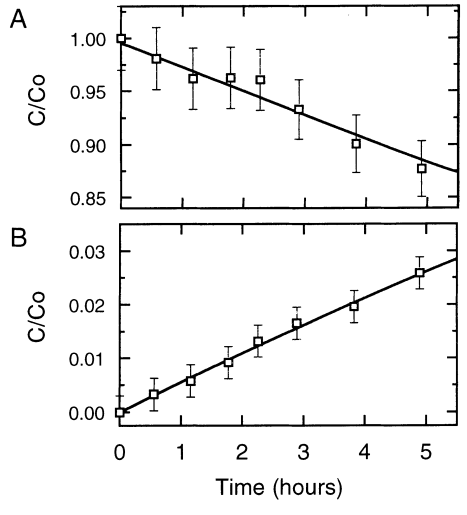

Fig. 5A,B Diffusion of tirapazamine under hypoxic conditions. The donating (**A**) and receiving (**B**) reservoir concentrations from one experiment are shown. Data were fitted simultaneously to a model to determine D and V_{max} *Error bars* indicate the estimated 3% fractional measurement error plus 0.003 constant error

standard deviation 0.4 μM/s ($n = 7$). For these experiments, there was a large amount of drug loss through tissue metabolism and the donating reservoir concentration was seen to decrease by 12% after 5 h while the receiving reservoir concentration increased by just 3% in the same time period.

Simulations

Modelling a tumour cord

Experimental results for the diffusion of tirapazamine through MCCs were used to model drug distributions within a cord of cells surrounding a blood vessel. To do this, a mathematical model was constructed which incorporated the estimates of the diffusion coefficient, D, and metabolic rate, V_{max}, along with other information regarding the tumour environment and the pharmacokinetics of tirapazamine.

Geometry and boundary conditions

Tumour geometry was modelled as being a cylindrical cord of cells with a radial thickness of 150 μm surrounding a blood vessel 10 μm in diameter. The cylindrical version of Eq. 1 is:

$$\frac{\partial C}{\partial t} = D\frac{\partial}{\partial r}\left(\frac{1}{r}\frac{\partial C}{\partial r}\right) - \frac{V_{max}C}{K'_m + C} \tag{3}$$

where 'r' is the radial distance into the tumour cord and K'_m is the Michaelis-Menten constant, K_m, modified to include the effect of oxygen-related competitive inhibition, which will be described below.

The condition for the blood vessel-tissue boundary was chosen to model the situation where the permeability of the endothelial wall was negligible, so that the first layer of tumour cells was exposed directly to the blood tirapazamine level. The blood concentration was held constant to reflect the clinical practice of administering tirapazamine by intravenous infusion over several hours [11]. Diffusion of tirapazamine beyond the outer layer of cells was modelled using a mirror blood vessel scheme, where drug diffusing out of the cord was matched by drug diffusing in from a mirror vessel.

Oxygen variation and tirapazamine metabolism

To complete the model, the rate of tirapazamine metabolism as a function of oxygen level and distance into the tumour cord must be considered. Oxygen partial pressure as a function of depth was modelled using a diffusion-reaction model for cylindrical geometry [1]:

$$pO_2(r) = pO_2\left[\frac{2\cdot\ln(r/r_{max}) + 1 - r^2/r_{max}^2}{2\cdot\ln(a/r_{max}) + 1 - a^2/r_{max}^2}\right] \tag{4}$$

where $pO_2(r)$ is the oxygen partial pressure as a function of radial distance from the centre of the blood vessel, pO_2 is the blood oxygen partial pressure ($r = 0$), a is the radius of the blood vessel and r_{max} is the distance where oxygen partial pressure falls to zero. For blood pO_2 values of 40, 20 and 10 mmHg, r_{max} was set to 150, 110 and 80 μm, respectively [1].

Using a competitive model for the effect of oxygen inhibition on tirapazamine metabolism, we obtain an expression for the variation of K'_m with pO_2 as follows:

$$K'_m = K_m\left(1 + \frac{pO_2}{K_{pO_2}}\right) \quad (5)$$

where K_{pO_2} is the oxygen partial pressure at which low-concentration tirapazamine metabolism is 50% inhibited. The value for K_{pO_2} was determined to be 4 ± 1 mmHg using published data for the exposure to tirapazamine, as a function of oxygen partial pressure required to achieve a 1% cell survival [13]. Using the Michaelis-Menten competitive inhibition equation, the value for K_{pO_2} implies a ratio of ~10 for the concentration of tirapazamine required to achieve equal cytotoxicity under oxic and hypoxic conditions (pO_2 is set equal to 40 mmHg oxic, and 0 mmHg hypoxic). If oxic levels are chosen to be 160 mmHg (20% oxygen) then the oxic/hypoxic cytotoxicity ratio becomes ~40 which is consistent with the reported value of ~38 for experiments done in air using human tumour cell lines [23]. Figure 6a shows the oxygen profile as a function of distance from a blood vessel and its effect on the metabolic rate, $V_{max}\,C/(K'_m + C)$, for at uniform tirapazamine distribution. In this case blood vessel pO_2 is set to 40 mmHg and tirapazamine concentration is fixed at 1 μ*M* throughout the tissue.

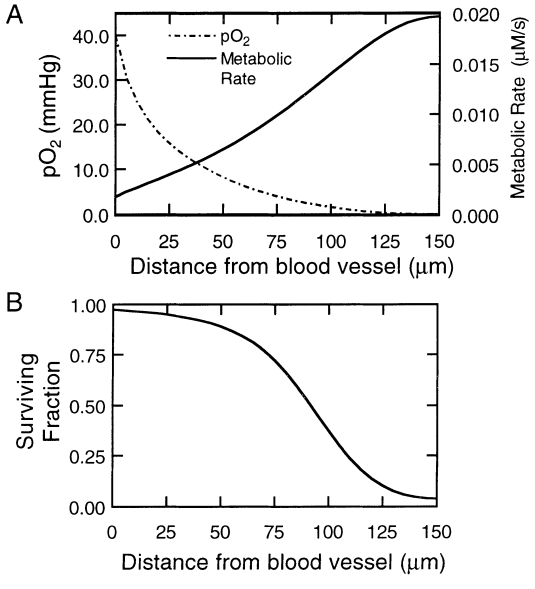

Fig. 6 A Variation of pO_2 and the metabolic rate with distance from a blood vessel. Functional dependence of pO_2 was obtained using Eq. 4. Variation of the metabolic rate followed a competitive inhibition model (Eq. 5) with K_{pO_2} set to 4 mmHg. Tirapazamine concentration, C, was set uniform throughout the cord at 1 μ*M*. **B** Simulated cell survival, as calculated using Eq. 6, from a 30-h exposure using the conditions of **A**

Relating tirapazamine exposure to cell survival

A relationship between the amount of tirapazamine metabolized and cell survival was obtained using published data for cell survival as a function of exposure to parent drug under hypoxic conditions [19]. The published data show a general trend for human cell lines which was averaged. In order to relate these results for exposure to tirapazamine under hypoxic conditions to exposure at any oxygen partial pressure, the amount of drug metabolized under the hypoxic conditions was calculated, yielding a direct link between the amount of drug metabolized and cell kill. The data for surviving fraction, now as a function of total metabolized drug (exposure), E, were then fitted to a sigmoidal function of the form:

$$SF = \frac{SF_0 - SF_\infty}{1 + e^{\frac{E - E_0}{\Delta E}}} + SF_\infty$$

where the model parameters were determined as follows; $SF_0 = 1$, $SF_\infty = -0.06$, $E_0 = 1.4$ m*M* and $\Delta E = 0.32$ m*M*. This relationship produced a good fit to the data for the range of accumulated metabolized drug exposures from 0 m*M* to 2.25 m*M*.

Simulations of tirapazamine distribution

Tumour cord drug distribution studies were carried out using Eqs. 3–6. Blood vessel tirapazamine levels were chosen to match the reported clinical level of ~5 μg/ml (30 μ*M*) which is achieved through intravenous infusion over several hours [11]. Figure 7a–c shows the results of simulations of the distribution of parent drug, metabolized drug and surviving fraction within the tumour cord. Each graph shows distributions at three different blood vessel partial pressures: 10, 20 and 40 mmHg. In each case, a stable drug gradient was seen to form within the tissue within approximately 15 min, at which point a balance was reached between drug influx from the blood vessel and drug loss through metabolism within the cord. The simulations of Fig. 7a indicate that the cells furthest from the blood vessel will see a maximum parent drug concentration of only ~10% that of the proximal cells. Figure 7b,c shows the net metabolized drug and resultant surviving fraction after a 4-h exposure. At blood pO_2 concentrations of 40 mmHg, very little cell kill occurs throughout the cord of cells, but when the blood pO_2 is reduced to 20 and 10 mmHg there is a significant increase in cytotoxicity towards cells proximal to the vessel but little toward the cells distal to blood vessels. The shaded regions, shown for the simulations at 40 mmHg, indicate the range of behaviour that the experimental uncertainity in D and V_{max} can produce. The boundaries of the shaded regions were determined

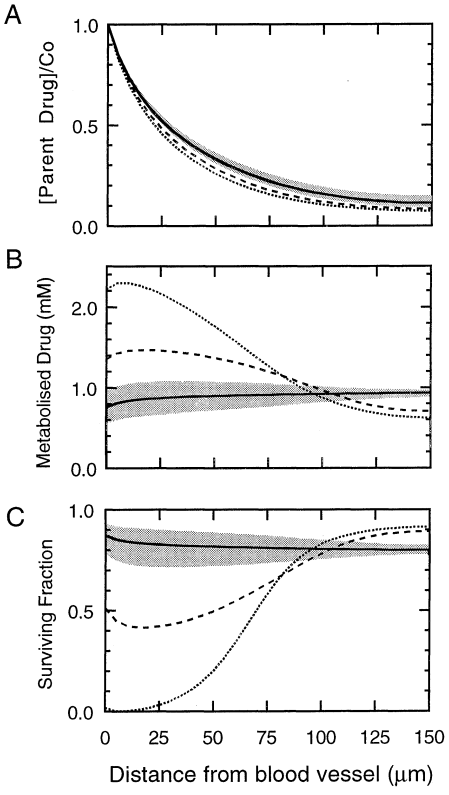

Fig. 7A–C Simulation of tirapazamine distribution within a tumour cord. Each graph **(A–C)** shows the results of simulations where the tirapazamine blood levels was kept at 30 μ*M* and blood pO_2 was set to 40 mmHg (- - -), 20 mmHg (—) and 10 mmHg (···) **A** shows the stable parent drug distribution which formed within 15 min. **B** shows the distribution of metabolized drug after a 4-h exposure under the conditions of A. **C** shows simulated cell kill as a function of distance from the blood vessel, calculated from the data of **B** using Eq. 6. The shaded regions shown for the simulations at 40 mmHg show the extent to which measurement error for D and V_{max} will modify the simulation results

by carrying out additional simulations, first with both D and V_{max} increased by one standard deviation and then with both parameters reduced by one standard deviation, as consistent with what occurred experimentally.

Discussion

Tirapazamine is a new bioreductive cytotoxin which exhibits selective toxicity toward cells at reduced oxygen tension. It could complement radiation therapy by killing radiation-resistant hypoxic cells [2] and chemotherapy by killing quiescent (non-cycling) cells located distal to tumour vasculature [7].

Measurements of tirapazamine flux through MCCs under oxic and hypoxic conditions were well fitted using the mathematical diffusion-reaction model. The diffusion parameter, D, is a measure of the effective diffusion coefficient of tirapazamine within MCCs composed of SiHa cells. It incorporates the net effect of drug diffusion through and around cells. While it would be expected to vary with changes of the cell environment, such as the fraction of extracellular space, no systematic variations with culture thickness were detected. The value of D_{Tira} was determined to be $7.0 \pm 0.5 \times 10^{-7}$ cm^2/s by taking the average of all results. The maximal metabolic rate, V_{max}, determines the rate that a fully hypoxic MCC metabolizes tirapazamine and was found to be 1.5 ± 0.4 μ*M*/s.

Measurements of the diffusion of tirapazamine under oxic and hypoxic conditions allowed us to simulate perivascular penetration of tirapazamine in an in vivo tumour cord. The simulations that were carried out using our estimates of diffusion and metabolism of tirapazamine illuminate the possible range of drug distributions expected to occur in a solid tumour. The microregional distribution of tirapazamine is governed by a balance between drug influx and oxygen-dependent drug metabolism. As tirapazamine diffuses away from blood vessels it is geometrically diluted and, as the oxygen tension decreases, metabolism increases. This metabolism generates a cytotoxic species which contributes to the antitumour effect, but also acts to consume and therefore hinder drug penetration. Overall, our simulations predicted that cells peripheral to blood vessels are exposed to only 10% of blood tirapazamine levels. As a result of this, little activity against hypoxic tumour cells residing distal to tumour blood vessels was predicted. Only when hypoxic cells reside close to the vasculature, for example as a result of depleted blood pO_2 at the end of tumour capillaries, did tirapazamine become significantly cytotoxic. This finding is consistent with experimental data from spheroids [9] and human xenografts and murine tumours [10] using flow cytometric sorting techniques. In the case of spheroids, under low oxygen tension, tirapazamine has been found to have minimal penetration and in animal systems employing SiHa xenografts or SCCVII tumours only a small differential in cell kill between the cells close to and distant from the vasculature is observed.

One possible method for improving drug penetration and cytotoxic exposure to peripheral cells would be to select a tirapazamine analogue which possesses a lower K_{pO_2} value, the oxygen partial pressure at which the rate of low-concentration tirapazamine metabolism drops to half its hypoxic rate. Figure 8a shows the results where K_{pO_2} was set to 1, 2 and 4 mmHg, other parameters were as in the simulations of Fig. 7a with $pO_2 = 40$ mmHg. These chosen values for K_{pO_2} translate to oxic versus hypoxic cytotoxicity ratios of ~40, 20 and 10, respectively. The simulations showed a moderate increase in drug distribution througout the cord, when K_{pO_2} was lowered from 4 mmHg to 1 mmHg, along with a substantial redistribution of metabolized drug and cytotoxic exposure. Hence a drug with a lower K_{pO_2} value would cause increased cell kill of peripheral cells while at the same time sparing cells close to blood vessels.

In summary, we used the in vitro MCC system, combined with mathematical modelling, to examine tumour drug distribution, and specifically characterized

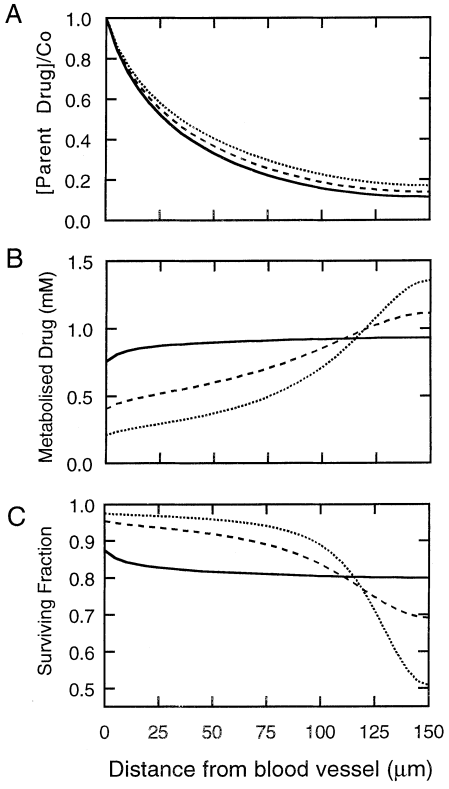

Fig. 8A–C Simulations in which the metabolic coefficient's dependency on oxygen partial pressure, K_{pO_2} was varied. Distributions are shown after a 4-h exposure at a 30 μ*M* blood tirapazamine level with pO_2 set to 40 mmHg and K_{pO_2} set to 4 mmHg (- - -), 2 mmHg (—) and 10 mmHg (· · ·) **A** shows the stable parent drug distribution which formed within 15 min. **B** shows the distribution of metabolized drug after a 4-h exposure under the conditions of **A**. **C** shows simulated cell kill as a function of distance from the blood vessel, calculated from the data of **B** using Eq. 6

the ability of tirapazamine to penetrate extravascular tumour tissue. We believe it would be possible to use a similar approach as a strategy to identify agents with clinical potential and propose that such a strategy could form an additional tool for drug discovery. The information obtained using the flux data from MCC experiments combined with simulations of tumour microarchitecture allow estimates to be made of drug effectiveness that cannot be obtained by conventional medicinal chemistry techniques employing physicochemical characteristics, in vitro activity and in vivo pharmacokinetic evaluation.

Acknowledgement Both authors would like to express their thanks to Karen H. Fryer, Peggy L. Olive and Ralph E. Durand for their helpful advice and assistance in completing this study.

References

1. Boag JW (1969) Oxygen diffusion and oxygen depletion problems in radiobiology. Curr Topics Radiat Res 5: 141
2. Brown JM (1993) SR 4233 (Tirapazamine): a new anticancer drug exploiting hypoxia in solid tumours. Br J Cancer 67: 1163
3. Brown JM, Lemmon MJ (1990) Potentiation by the hypoxic cytotoxin SR 4233 of cell killing produced by fractionated irradiation of mouse tumours. Cancer Res 50: 7745
4. Brown JM, Lemmon MJ (1991) SR 4233 – a tumor specific radiosensitizer active in fractionated radiation regimes. Radiother Oncol 20: 151
5. Cowan DSM, Hicks KO, Wilson WR (1996) Multicellular membranes as an in vitro model for extravascular diffusion in tumours. Br J Cancer 74: S28
6. Crank J (1975) The mathematics of diffusion. Clarendon Press, Oxford
7. Dorie MJ, Brown JM (1993) Tumor-specific, schedule-dependent interaction between tirapazamine (SR 4233) and cisplatin. Cancer Res 53: 4633
8. Durand RE (1994) The influence of microenvironmental factors during cancer therapy. (review, 120 refs). In Vivo 8(5): 691
9. Durand RE, Olive PL (1992) Evaluation of bioreductive drugs in multicell spheroids. Int J Radiat Oncol Biol Phys 22: 689
10. Durand RE, Olive PL (1997) Physiologic and cytotoxic effects of tirapazamine in tumor-bearing mice. Radiat Oncol Invest 5: 213
11. Graham MA, Senan S, Robin H Jr, Eckhardt N, Lendrem D, Hincks J, Greenslade D, Rampling R, Kaye SB, Roemeling R von, Workman P (1997) Pharmacokinetics of the hypoxic cell cytotoxic agent tirapazamine and its major bioreductive metabolites in mice and humans: retrospective analysis of a pharmacokinetically guided dose-escalation strategy in a phase I trial. Cancer Chemother Pharmacol 40(1): 1
12. Hicks KU, Ohms SJ, Zijl PL van, Denny WA, Hunter PJ, Wilson WR (1997) An experimental and mathematical model for the extravascular transport of DNA intercalator in tumours. Br J Cancer 76(7): 894
13. Koch CJ (1993) Unusual oxygen concentration dependence of toxicity of SR-4233, a hypoxic cell toxin. Cancer Res 53(17): 3992
14. Laderoute K, Wardman P, Rauth AM (1988) Molecular mechanisms for the hypoxia dependent activation of 3-amino-1,2,4-benzotriazine-1,4-dioxide (SR 4233). Biochem Pharmacol 37: 1487
15. Minchinton AI, Wendt KR, Clow KA, Fryer KH (1997) Multilayers of cells growing on a permeable support: an in vitro tumour model. Acta Oncol 36: 13
16. Olive PL, Durand RE (1994) Drug and radiation resistance in spheroids: cell contact and kinetics (review, 146 refs). Cancer Metastasis Rev 13(2): 121
17. Press WH (1992) Numerical recipes in C: the art of scientific computing. Cambridge University Press, Cambridge
18. Senan S, Rampling R, Wilson P, Lawson N, Robin H, Murray LS, Workman PMG, Kaye SB (1994) Phase I and pharmacokinetic study of tirapazamine (SR 4233), a highly selective hypoxic cell cytotoxin. Ann Oncol 5 [Suppl 5]: 135
19. Siim BG, Ziji PI van, Brown JM (1996) Tirapazamine-induced DNA damage measured using the comet assay correlates with cytotoxicity towards hypoxic tumour cells in vitro. Bri J Cancer 73(8): 952
20. Sutherland RM (1988) Cell and environment interactions in tumor microregions: the multicell spheroid model. Science 240: 177
21. Thomlinson RH, Gray LH (1955) The histological structure of some human lung cancers and the possible implications for radiotherapy. Br J Cancer 9: 539
22. Wang, J Biedermann KA, Wolf CR, Brown JM (1993) Metabolism of the bioreductive cytotoxin SR 4233 by tumour cells: enzymatic studies. Br J Cancer 67: 321
23. Zeman EM, Brown JM, Lemmon MJ, Hirst VK, Lee WW (1986) SR-4233: a bioreductive agent with high selective toxicity for hypoxic cells. Int J Radiat Biol Phys 12: 1239
24. Zeman EM, Hirst VK, Lemmon MJ, Brown JM (1988) Enhancement of radiation-induced tumor cell killing by the hypoxic cell toxin SR-4233. Radiother Oncol 12: 209